Journal of Photochemistry and Photobiology B: Biology xxx (2015) xxx–xxx

Contents lists available at ScienceDirect

Journal of Photochemistry and Photobiology B: Biology

journal homepage: www.elsevier.com/locate/jphotobiol

Urea enhances the photodynamic efficiency of methylene blue

Silvia C. Nuñez [a], Tania M. Yoshimura [a], Martha S. Ribeiro [a], Helena C. Junqueira [b], Cleiton Maciel [c], Maurício D. Coutinho-Neto [c], Maurício S. Baptista [b,*]

[a] Centro de Lasers e Aplicações, IPEN-CNEN/SP, Av. Lineu Prestes, 2242, São Paulo, SP 05508-000, Brazil
[b] Departamento de Bioquímica, Instituto de Quimica, Universidade de São Paulo, AV prof. Lineu Prestes, 748, São Paulo, SP 05508-000, Brazil
[c] ABCSim, Centro de Ciências Naturais e Humanas, Universidade Federal do ABC, Rua Santa Adélia 166, Santo André, SP 09.210-170, Brazil

ARTICLE INFO

Article history:
Received 16 November 2014
Received in revised form 28 February 2015
Accepted 19 March 2015
Available online xxxx

ABSTRACT

Methylene blue (MB) is a well-known photosensitizer used mostly for antimicrobial photodynamic therapy (APDT). MB tends to aggregate, interfering negatively with its singlet oxygen generation, because MB aggregates lean towards electron transfer reactions, instead of energy transfer with oxygen. In order to avoid MB aggregation we tested the effect of urea, which destabilizes solute–solute interactions. The antimicrobial efficiency of MB (30 μM) either in water or in 2 M aqueous urea solution was tested against a fungus (*Candida albicans*). Samples were kept in the dark and irradiation was performed with a light emitting diode (λ = 645 nm). Without urea, 9 min of irradiation was needed to achieve complete microbial eradication. In urea solution, complete eradication was obtained with 6 min illumination (light energy of 14.4 J). The higher efficiency of MB/urea solution was correlated with a smaller concentration of dimers, even in the presence of the microorganisms. Monomer to dimer concentration ratios were extracted from the absorption spectra of MB solutions measured as a function of MB concentration at different temperatures and at different concentrations of sodium chloride and urea. Dimerization equilibrium decreased by 3 and 6 times in 1 and 2 M urea, respectively, and increased by a factor of 6 in 1 M sodium chloride. The destabilization of aggregates by urea seems to be applied to other photosensitizers, since urea also destabilized aggregation of Meso-tetra(4-n-methyl-pyridyl)porphyrin, which is a positively charged porphyrin. We showed that urea destabilizes MB aggregates mainly by causing a decrease in the enthalpic gain of dimerization, which was exactly the opposite of the effect of sodium chloride. In order to understand this phenomenon at the molecular level, we computed the free energy for the dimer association process (ΔG_{dimer}) in aqueous solution as well as its enthalpic component in aqueous and in aqueous/urea solutions by molecular dynamics simulations. In 2 M-urea solution the atomistic picture revealed a preferential solvation of MB by urea compared with MB dimers while changes in ΔH_{dimer} values demonstrated a clear shift favoring MB monomers. Therefore, MB monomers are more stable in urea solutions, which have significantly better photophysics and higher antimicrobial activity. This information can be of use for dental and medical professionals that are using MB based APDT protocols.

1. Introduction

Photodynamic antimicrobial therapy (APDT) is an important alternative approach to treat microbial diseases, overcoming the dangerous emergent microbial resistance [1]. The absence of reported microbial resistance makes APDT an important tool to be used in medicine and dentistry [1,2].

The principle of APDT is the light activation of a compound, known as photosensitizer (PS) that causes photooxidation of biomolecules by two main mechanisms, which are type I and type II. In type I, there is an initial PS-substrate (biomolecules) reaction leading to the formation of radicals and subsequently several reactive oxygen species (ROS), as the extremely reactive hydroxyl radical. In type II the initial step is an energy transfer reaction from the PS triplet state to molecular oxygen, leading to the formation of singlet oxygen, which is a highly reactive oxygen species [3]. Depending on the PS concentration, its ground state may also work as an electron donor, allowing electron transfer reactions that can either destroy the PS or allow the formation of other ROS (dye-dye mechanism).

Many photosensitizers (PSs) are currently being tested and used as antimicrobial agents [4]. Because the membranes of microorganisms are always negatively charged, the positively charged PSs attach and/or penetrate more efficiently to/in them and end up working better in APDT. Among the positively charged PSs,

* Corresponding author.

http://dx.doi.org/10.1016/j.jphotobiol.2015.03.018
1011-1344/

methylene blue (MB) is one of the most used in experimental work and in clinical applications in dentistry and medicine [2,5,6].

MB is a cationic dye that efficiently absorbs in the red (ε 10^5 M^{-1} cm^{-1} at λ = 664 nm). It is also a metachromatic compound, which means that its absorption spectrum is concentration-dependent. MB forms dimers or higher aggregates in solution upon increasing dye concentration; therefore Beer's law is not obeyed. The extinction coefficient at λ = 664 nm diminishes and it increases around λ = 610 nm (dimer band) with the increase in dye concentration. Dimerization increases at higher ionic strength and may also change in the presence of charged interfaces, depending on the ratio between dye and interface [7–9]. MB monomers and dimers present different photochemical behavior. MB aggregates lean towards electron transfer reactions (dye–dye mechanism), while monomers tend to engage in energy transfer reactions (type II) [9]. In a recent work, we observed a reduced antimicrobial activity for MB with a slight increase in the ionic strength of MB solutions, i.e., 0.9% of NaCl [10]. We perceived a decrease in singlet oxygen production that significantly impaired MB antimicrobial activity.

Since the control of the ionic strength is not feasible in biological media, we started to look for means to overcome this effect, and decided to test the addition of urea to the MB solution. The effect of urea as a modifier of water solutions have usually been interpreted as arising from a direct (water replacement) or indirect mechanism related to a decrease in solvation entropy of water/urea mixtures [11]. Urea weakens hydrophobic bonds, changes the dielectric constant and increases the surface tension of water, which usually causes a decrease in substrate–substrate interactions, such as those found in ion-pairs [12–14]. An earlier investigation showed the ability of urea to promote MB disaggregation [12], however, the molecular understanding of this effect is still not known and this effect was never studied as a way to improve the photodynamic efficiency of MB towards a more potent antimicrobial agents.

Therefore, the purpose of this work is to investigate MB/urea aqueous solutions in terms of the photochemical behavior and its antimicrobial activity against *Candida albicans* and to compare these results with simple water solutions. We also wanted to exploit and understand the molecular mechanism involved in the decrease of MB aggregates by urea. We start by presenting the antimicrobial data and in the second part of the paper we provide experimental and theoretical data explaining, at the molecular level, the effect of urea on MB aggregation. Molecular dynamics simulations were employed to enable a microscopic view of the effects of urea on MB aggregation. Comparison between experimental and theoretical results for the association free energy was performed using Thermodynamic Integration (TI) techniques.

2. Material and methods

2.1. Reagents

All solvents were of spectroscopic grade. Water was bi-distilled from an all glass apparatus and was further purified via a millipore Milli-Q system (resistivity smaller than 18 MΩ cm). Urea was recristalized from methanol. Methylene Blue (MB) and Meso-tetra(4-n-methyl-pyridyl)porphyrin (TMPyP) were acquired from Sigma–Aldrich and used as received.

2.2. Strain and inoculum preparation

Suspensions of *C. albicans* (ATCC 90028) cells in exponential phase were obtained after 8 h growth in Sabouraud (Sb) dextrose broth, incubated in a biological shaker at 37 °C. Cells were washed twice and suspended in distilled water, with standardized concentration of 10^6 colony forming units per milliliter (CFU/mL) after setting the suspension transmittance by 60% at λ = 540 nm (Spectrophotometer SP220, Biospectro, Brazil).

2.3. Effect of urea in APDT

In order to verify the viability of *C. albicans* in water or urea solutions, two environmental control groups were set (Table 1). Another two control groups were prepared to evaluate dark toxicity of MB in aqueous or in urea solutions (see Table 1). Commercially available MB (Sigma–Aldrich, USA) was dissolved in water to a stock concentration of 120 μM. Urea (Sigma–Aldrich, USA) was dissolved in water to a stock concentration of 8 M. All control preparations were placed in a sterile 96-well microwell plate, and were kept during the entire microbiological experiment resting in the dark. Thereafter, they were ten-fold serially diluted in water and 10 μL aliquots of each dilution were plated on Sb agar using the track-dilution method [15]. Plates were incubated for 18 h at 37 °C, and the colony forming units were counted and converted into CFU/mL values.

After the controls setting, we prepared two treatment groups: Treatment Group Distilled Water and Treatment Group Urea as showed in Table 2. The experimental mixtures were kept in dark for 5 min and then the irradiation was performed with a light emitting diode (LED) with λ = 645 nm ± 10 nm (prototype, MMOptics, São Carlos, Brazil), exposure time of 3, 6 or 9 min, which is equivalent to energies of 7.2, 14.4, and 21.6 J and light doses of 18, 36, and 54 J cm^{-2}, respectively. Total output power of 40 mW was verified using an appropriate power meter (Scientech 373, Boulder Corp, USA). The LED probe was fixed on a holder that kept the beam area at 0.4 cm^2, which coincided to a single well size from the 96-well microwell plate. After each treatment, the groups were ten-fold serially diluted in PBS and aliquots (10 μL each) were plated on

Table 2
Experimental groups.

Treatment groups	Inoculum (10^6 CFU/mL)	Diluent volumes			Final concentration	
		Water	Urea 8 M	MB 120 μM	Urea	MB
Distilled water	100 μL	50 μL	–	50 μL	0	30 μM
Urea		–	50 μL	50 μL	2 M	30 μM

Table 1
Experimental control groups.

Control groups	Inoculum (10^6 CFU/mL)	Diluent volumes			Final concentration	
		Water	Urea 8 M	MB 120 μM	Urea	MB
Distilled water (C)	100 μL	100 μL	–	–	0	0
Urea (UC)		50 μL	50 μL	–	2 M	0
MB toxicity		50 μL	–	50 μL	0	30 μM
MB + urea toxicity		-	50 μL	50 μL	2 M	30 μM

Please cite this article in press as: S.C. Nuñez et al., Urea enhances the photodynamic efficiency of methylene blue, J. Photochem. Photobiol. B: Biol. (2015), http://dx.doi.org/10.1016/j.jphotobiol.2015.03.018

Sb agar using the track-dilution method abovementioned. Plates were incubated to obtain the CFU/mL values after 18 h at 37 °C. The irradiation parameters were chosen to allow an identification of possible difference between groups; therefore, a moderate reduction was expected. All microbiological experiments were conducted in triplicates, and repeated among two different experimental days, which totalized $n = 6$ for all groups.

2.4. Microbiological data analysis

Fungi reduction is presented as survival fraction. Cell viabilities were monitored through counting colony forming units on agar plates. The data were statistically analyzed firstly by Shapiro–Wilk test to verify normal distribution of the samples. Thereafter, we performed One-way Analysis of Variance (ANOVA) test followed by Tukey test with the significance level accepted at 5% ($p < 0.05$). According to our microbiological results we decided to pursuit an investigation on some variables that might have been responsible for the observed effects mostly regarding MB aggregation on both solutions

2.5. Optical characteristics of the photosensitizers

The optical characteristics of the dye in the APDT assays were obtained through absorbance spectra in a computer-interfaced spectrophotometer of multichannel optical design (SpectraMax M4, Molecular Devices, USA) in 96 wells plate. The dye spectra for the calculation of dimerization constants were recorded in a Shimadzu UV-2400-PC, using 1 or 0.1 cm optical path length quartz cuvettes. Spectral data were further manipulated with a 386 GRAMS software (Galatic, Inc). Fluorescence emission measurements were performed on a Spex FLUOROG spectrofluorometer. *C. albicans* suspensions were prepared to obtain a final fungal concentration of approximately 10^6 CFU/mL and 30 μM-MB. Spectra were recorded after 5 min of contact time. Appropriate dilutions were prepared to obtain the same final concentrations as presented in Table 2. Spectra were analyzed regarding dimer and monomer ratio according to the following formula for MB: $R\left[\frac{DA}{MA}\right] = A610\,nm/A660\,nm$, were R means the ratio; DA, dimer absorption (±610 nm), and MA monomer absorption (±660 nm) [7]. The temperature of the cuvette holder was controlled by a water bath.

The dimerization constants were obtained by fitting the absorbance data as a function of concentration, using the equilibrium equation and the boundary conditions (Eqs. (1)–(3).

$$M + M \rightleftharpoons D \tag{1}$$

$$[D] = (C_T - [M])/2 \tag{2}$$

$$Abs\ (660\,nm) = \varepsilon_{(M)} \cdot l \cdot [M] + \varepsilon_{(D)} \cdot l \cdot [D] \tag{3}$$

where $\varepsilon_{(M)}$ and $\varepsilon_{(D)}$ are molar absorptivity of monomers and dimers, respectively, l is the cuvette path length (1 cm), [M] and [D] are the monomer and dimer equilibrium concentrations and C_T is the total MB concentration. Gibbs free energy was obtained directly from the equilibrium constants. The enthalpic and entropic terms of the equilibrium constants were obtained by performing experiments at different temperatures and calculating the respective contributions of these terms in Vaŕt Hoff plots.

2.6. Computation details

Cubic cells of simulations containing monomers and dimers of MB in solution were modeled using a 2 M concentration of urea. The simulations were performed in the isothermic–isobaric ensemble (NPT) under room conditions, where the pressure ($p = 1$ atm) and the temperature ($T = 298$ K) were kept constant by using the parrinello–Rahman [16] and v-rescale schemes [17]. The simple charge model (SPC) [18] was the potential used to represent the water in the simulations. The reference geometries for MB in monomeric and dimeric forms were obtained using the BLYP functional [19,20] augmented with DCACP [21] corrections for describing weak interactions [22]. An anti-stacked geometry was selected as the lowest energy among the possible stacked configurations. Partial atomic charges were determined using the ChelpG method [23] using the B3LYP functional [19,20,24] and the 6-311G + (d) basis set [25]. Computational cells were previously equilibrated for 1 ns. The thermodynamic properties were calculated after a production molecular dynamics (MD) phase of 10 ns. The bond lengths were constrained using LINCS algorithm [26]. A cut-off of 1.2 nm was applied in the van der Waals interactions. The electrostatic interactions were treated by Particle Mesh Ewald (PME) method [27]. Computational simulations of MB^+ combined with the thermodynamic integration (TI) method [28] were employed to obtain the solvation free energies in monomeric and dimeric forms in aqueous solutions. Enthalpic contributions were computed from 10 ns trajectories while a cutoff of 1.2 nm was used for computing individual contributions to ΔH_{dimer}. Dimers were constrained to their equilibrium DFT geometry using a harmonic potential with constant applied to all atoms. Running lengths of 5 ns were performed in production phase for each integration window of length 0.1. Free energy calculations and molecular dynamics were performed using the GROMACS 4.5. program [29,30]. Quantum calculations for geometry optimization and partial charge were performed with Gaussian 09 [31,32].

3. Results and discussion

3.1. APDT with MB in the presence of uea

Microbial reductions obtained on the different tested conditions (Tables 1 and 2) are presented on Fig. 1A. The addition of 2 M urea to the solution did not affect the viability of *C. albicans* ($p = 0.99$) by itself. APDT was effective enough to cause a significant reduction of microorganisms in all tested conditions.

Even with 3 min of irradiation the fungal burden obtained in aqueous and urea solutions were significantly different ($p = 0.004$), with the MB/urea solution presenting a more expressive reduction of about 80%, although the reduction was next to the same log count. On the other hand, after 6 min of irradiation the solution of MB/urea obtained a complete eradication of 6 logs (100%). Comparing the results of MB alone and MB with urea with the same irradiation time we obtained a significant statistical reduction ($p = 0.0002$) in favor of MB/urea solution. To obtain the same 6 log reduction with aqueous MB solution was necessary to irradiate more 3 min, which gives a total of 9 min of irradiation and 21.6 J compare to 14.4 J for MB/urea solution.

Reports on the literature using *C. albicans* suspension and MB concentrations ranging from 70.4 μM to 130 μM showed reductions of about 75% on cell counts while our study with MB and urea showed 100% of reduction [33–35]. In fact, Prates et al. using the same strain (ATCC 90028) reached a reduction of about 1 log after 6 min of APDT with MB using very similar light parameters [36]. Therefore, it is clear that MB:urea solutions could be used in the development of more efficient APDT protocols. However, before developing any translational clinical research of these results, it is important to perform dark/light toxicity assays in eukaryotic cells, as well as, to understand the mechanism by which urea enhances the efficiency of MB in APDT protocols. In our study MB:urea solutions showed no dark toxicity to *C. albicans* cells,

Please cite this article in press as: S.C. Nuñez et al., Urea enhances the photodynamic efficiency of methylene blue, J. Photochem. Photobiol. B: Biol. (2015), http://dx.doi.org/10.1016/j.jphotobiol.2015.03.018

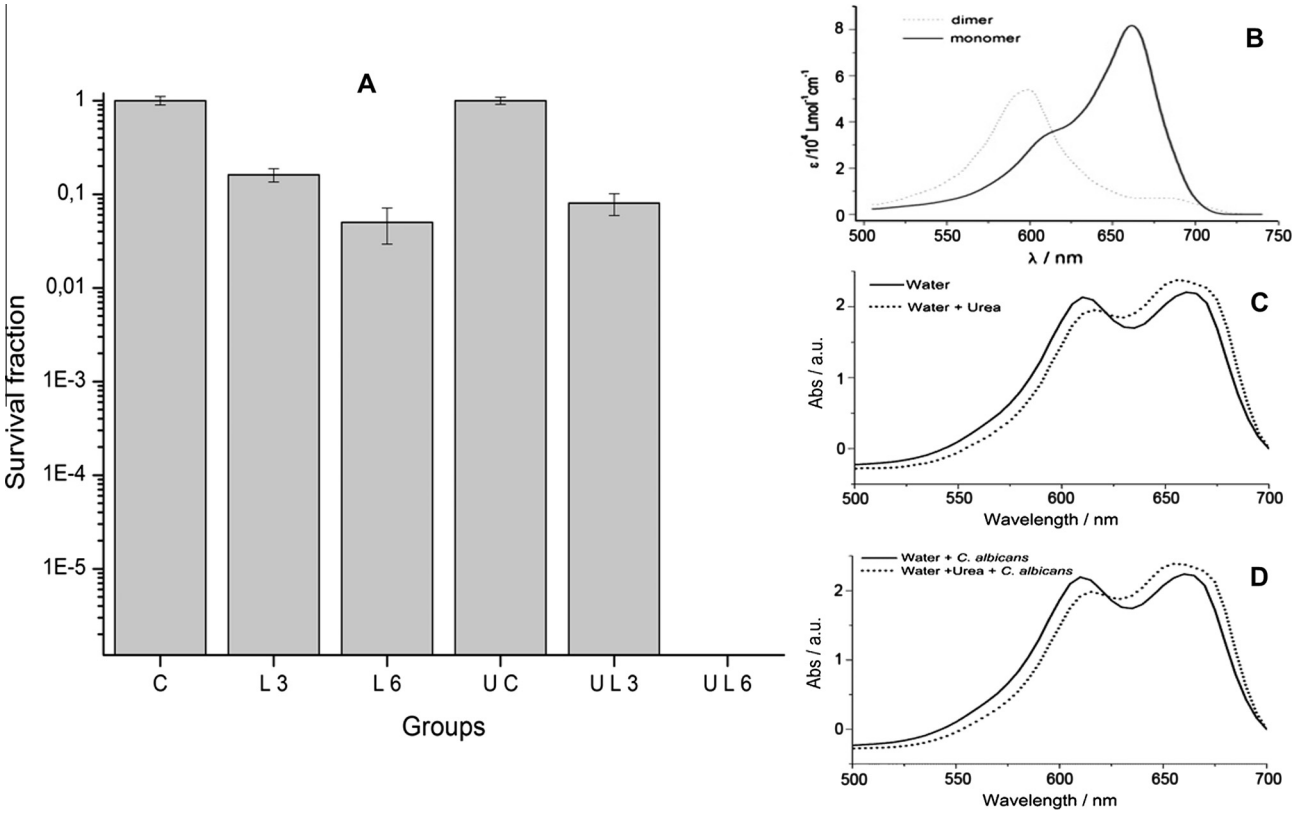

Fig. 1. Survival fraction on APDT assays and MB aggregation. (A) APDT effective reduction of *C. albicans*: C and UC are control samples of 30 μM MB in water and in 2 M urea solutions, respectively, without irradiation. L3, L6, UL3, UL6 are cell counts after 3 and 6 min of irradiation of 30 μM MB in water and in 2 M MB/urea solutions. For irradiation conditions see Materials and Methods. (B) Electronic absorption spectra of dimer and monomer species of methylene blue in water. (C) Absorption spectra of a 30 μM MB solution in water and in 2 M of urea. (D) Absorption spectra of a 30 μM MB solution in water and in 2 M of urea in the presence of *C. albicans* (10^6 CFU/mL).

but the study of the light toxicity in mammalian cells will be considered in another publication. Below we will focus on the mechanism of urea action.

In Fig. 1B and C one can observe the effect of urea (2 M) on the absorption of a 30 μM MB solution in the absence and presence of fungi, respectively. Note that in the absence of urea in both cases (presence or absence of fungi) the absorption at $\lambda = 660$ nm (monomer peak, M) is almost the same as the absorption at $\lambda = 600$ nm (dimer peak, D). The D/M ratio was close to 1 in the presence and absence of fungi. However, in the presence of urea, D/M ratio decreases both in the absence and presence of fungi, reaching a D/M value of ~0.8. This change of D/M ratio from 1 to 0.8 in the absence and presence of urea, respectively, was also observed at 30 μM MB solutions. Therefore, even in the presence of *C. albicans* we see the disaggregation tendency of MB in the presence of urea. The disaggregation tendency of MB in the presence of urea is therefore quite clear. Considering that the effect of urea could be used in connection with several photosensitizers, i.e. not only with MB, it is interesting to study with further details this phenomenon.

3.2. Effect of urea on the MB aggregation equilibrium

As mentioned in the introduction, the absorption spectrum of MB solution changes as a function of concentration and therefore at hardly any condition the absorbance at a specific wavelength follows a straight line with concentration, i.e., Beeŕs law is basically not followed (Fig. 2 A, C and E). Note also that the deviations from linearity are larger at higher concentrations and follows the trend NaCl > water > urea. These deviations are because of dye aggregation, which is favored in NaCl and avoided in urea solutions. The fact that NaCl increases aggregation is related with the screening of the electrostatic repulsion between two methylene blue molecules [7–10]. The reason why urea decreases aggregation is the main focus of this work. As the aggregation tendency increases at lower temperatures, it indicates that this equilibrium is driven by enthalpy and not by entropy (see further analysis below). It is also evident that aggregation increases in salted and decreases in urea solutions, as expected.

The values of the dimerization constants (K_D) were plotted as a function of $1/T$ for water, 1 M urea and NaCl solutions (Fig. 2B, D and F). Note that in all cases, it was possible to fit the variables to a straight line and to calculate the entropic and enthalpic values of the aggregation reactions (Table 3). The fact that the Vaṅt Hoff plots have positive slopes indicates the endothermic nature of the reaction, proving that MB dimerization is enthalpic driven. The entropic term is negative, indicating that the dimerization is not driven by entropy. Note also that K_D decreases from 4.7 to 1.6×10^3 M, going from water to urea 1 M. There is a further decrease in K_D to 0.8 M in 2 M urea solution ($\Delta G = -16.5$ kJ mol^{-1} at this condition). The decrease in ΔG comparing water to 2 M urea solution is 4.4 kJ mol^{-1}. Therefore, this proves the shift in the MB dimerization equilibrium favoring monomers in urea solutions. The opposite effect is observed for NaCl solutions, i.e., a considerable increase in K_D (~6 times, Table 3). Note also that the enthalpic gain of dimerization is decreased in the presence of urea and increased in the presence of NaCl. This data suggests that urea solutions solvate better the monomers and NaCl solutions solvate better the dimers. At very much larger urea concentrations (5 and 6 M) there is reversion in the signal of the dimerization equilibrium constants and the Gibbs free energy of aggregation becomes positive, i.e. MB aggregation is largely improbable at 6 M urea (Fig. 3). At these high urea concentrations, there are

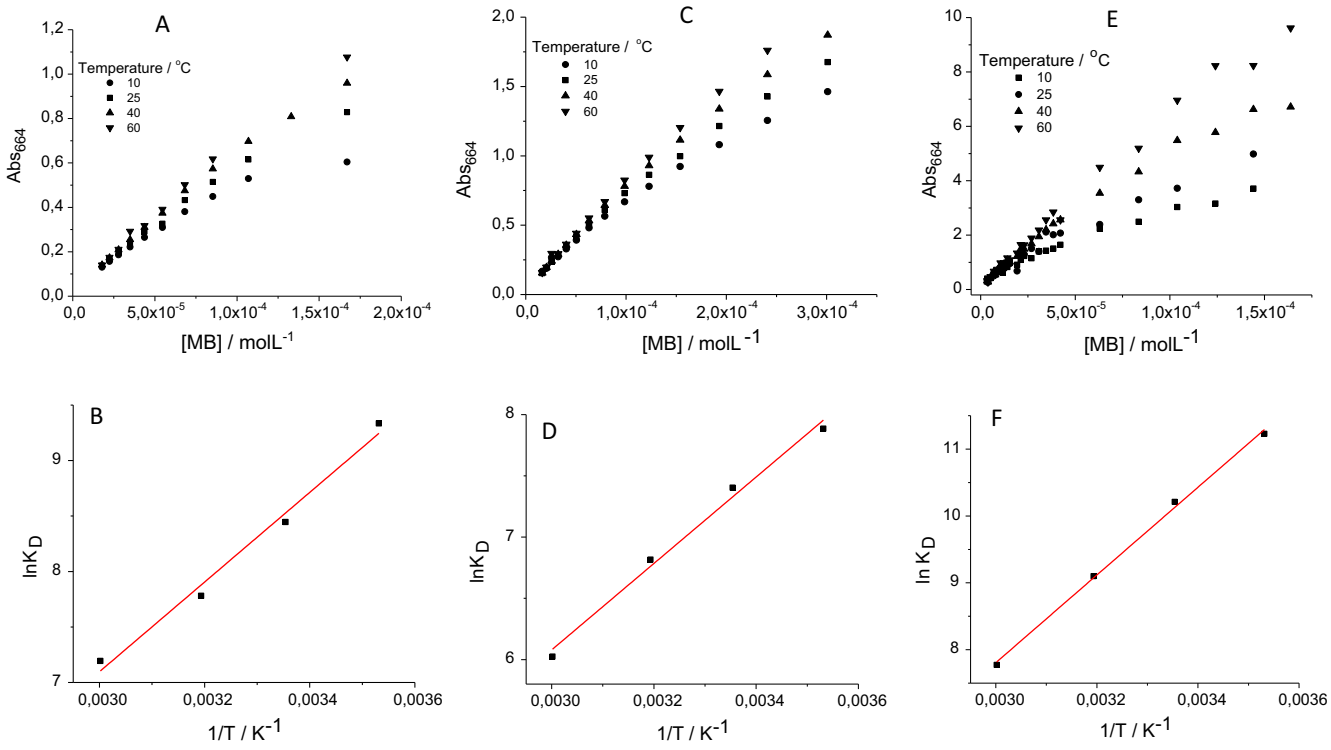

Fig. 2. Effect of sodium chloride and urea on the absorption spectra of MB. Absorbance at $\lambda = 664$ nm of MB solutions as a function of MB concentration at different temperatures in aqueous solution (A), in 1 M urea (C) and in 1 M sodium chloride (E). Vaṅt Hoff plots ($\ln K_D$ versus $1/T$) of MB in aqueous solution (B), in 1 M urea (D) and in 1 M sodium chloride (F).

Table 3
Dimerization constants (M) and Gibbs free energy at $T = 298.15$ K, and enthalpy and entropy changes (kJ mol^{-1}).

Solution	K_D ($\times 10^{-3}$)	ΔG	ΔH	$T\Delta S$
Water	4.7	−20.9	−33.6	−12.7
Urea (1 M)	1.6	−18.3	−29.3	−11.0
NaCl (1 M)	27.2	−25.3	−54.5	−29.2

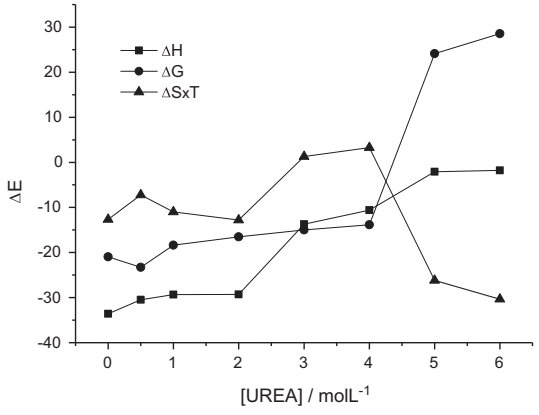

Fig. 3. Effect of urea on the thermodynamic parameters (ΔG, ΔH, $T\Delta S$) of aggregation as a function of urea concentration.

several other effects that can occur in cells by the sole presence of high urea concentration, and we decided to only test APDT at 2 M.

In order to study the mechanism of urea on decreasing MB aggregation with further molecular details we relied on molecular dynamics simulations. A clear preferential solvation effect of urea to both monomeric and dimeric forms of MB was observed (Fig. 4).

In fact, urea tends to solvate better MB hydrophobic portions such as the sulphur atom and the methyl groups (Fig. 4). Although it also solvates dimer species, the urea coverage of MB dimers is smaller. Integration of the number of molecules over the first solvation shell revealed that the proportion of urea molecules is non-statistically close to MB at 2 M, having 5 molecules of urea and 46 molecules of water for the monomer and 5 molecules of urea and 44 molecules of water for the dimer.

The free energy computed using TI for the dimer formation process in water at 298 K produces a value of −114.9 kJ mol^{-1} for ΔG_{dimer}, with ΔH_{dimer} and $T\Delta S_{dimer}$ being −91.2 and 23.7 kJ mol^{-1} respectively. These values are in line with the ones computed for the same process using several distinct solvation methods [22] and reproduce the experimental finding that dimerization in water is mostly driven by enthalpy. Direct comparison with the experimental ΔG_{dimer} is not possible as our result includes only contributions coming from changes in solvation free energy upon dimerization, lacking all contributions from specific MB^+–MB^+ interactions.

Calculations for the $\Delta\Delta H_{dimer}$ shift when adding urea revealed a clear enthalpic contribution of 14.0 kj mol^{-1} favoring the monomer. This effect is qualitatively but not quantitatively correct since solution thermodynamic experiments at the same 2 M concentration produces a $\Delta\Delta H_{dimer}$ of only 4 kJ mol^{-1}. However, changes of 19.9 kl mol^{-1} observed at 3 M are much closer to the ones computed at 2 M suggesting that the employed methodology overestimates urea's destabilization effects on MB aggregation. Limitations of the force field used, especially lack of explicit polarization, might be the culprit for the overestimation as the MB dimer should induce a stronger polarization on the solvent. Looking at individual enthalpic contributions to ΔH_{dimer} (Table 4) revealed that the short-range contributions to ΔH_{dimer} arising from MB^+ interacting directly with the solvent are relevant but do not show the whole picture. In fact, the dimer destabilization arises

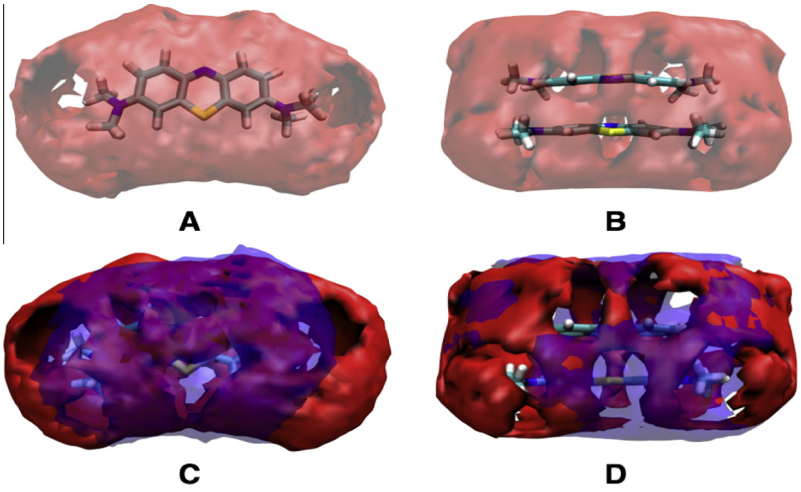

Fig. 4. Spatial distribution function for water (red) and urea (blue) computed with respect to the center of mass of the molecules with respect to MB. Averages were taken over a 10 ns simulation. Dimers are in an *anti*-configuration as mentioned in the text. Panels A and B are for the water only monomer and dimer respectively while C and B are results for 2 M of urea. (For interpretation of the references to color in this figure legend, the reader is referred to the web version of this article.)

Table 4
Short and long range enthalpic changes (kJ mol^{-1}) upon dimerization for specific ΔH_{dimer} components from molecular dynamics simulations. Averages were taken from 20 ns runs after equilibration using a cutoff of 12 Å for computing short-range interactions. MB stands for Methylene Blue, Sol for Solvent. Ref-Vac stands for the change in electrostatic energy upon dimerization in vacuum.

ΔH_{dimer}					
Solution	MB-Sol	Sol–sol	Long-range	Ref-Vac	Total
Water	−0.3	42.0	25.3	−159.9	−92.9
Urea 2 M	13.1	15.5	52.4	−159.9	−78.9

from a less efficient compensation of effects upon dimerization for a water-urea mixture when compared to pure water, especially for the long-range component. That is, from an enthalpic point of view, solvating the dimer is less efficient then solvating the monomers in a water/urea mixture when compared to water.

3.3. Will urea affect the monomer dimer equilibrium of other dyes?

Usually the aggregation of charged organic dyes in aqueous solutions is driven by enthalpy changes and urea can potentially decrease the tendency to form these aggregates. In fact, we have observed that the photophysical properties of several dyés solutions are affected by the presence of urea. Clear metachromatic changes are observable for phenothiazinium salts, which are expected, since they all have similar structure to that of MB. However, this effect may also work for other lead compounds such as porphyrins. Although this publication focuses mainly on the effect of urea on MB aggregation, in order to show an initial data on the effect of urea in disaggregating other PSs, we obtained the absorption and emission spectra of TMPyP in water and 2 M urea solutions (Supplementary Fig. 1). The absorption maxima have small red shifts (1–3 nm) and the emission spectra, which is split in two maxima at 670 and 710 nm, has a substantial increase in the emission integral (12.5%), in the presence of urea. Note also the clear increase in the relative area of the 670 nm peak. These three changes, red shift, increase in fluorescence emission and increase in the 670 nm peak, are indicative of disaggregation [37]. Therefore, it is likely that urea also decreases the tendency of aggregation of other PSs, although it is necessary to test this concept with more detail with other molecules. We hope this work will stimulate further research on this area.

4. Conclusion

Urea stabilizes solution monomers (and consequently reduces dimer concentration) of MB allowing more efficient APDT on *C. albicans* and it is likely that this observation is valid for other PSs as well. Considering the low cost of urea and its low toxicity, the addition of urea to aqueous formulations of photosensitizers could improve their efficiency. It is important to acknowledge that more studies are needed to establish the safety of urea use in clinical APDT protocols.

Acknolegedments

M.D. Coutinho-Neto would like to thank L.G. Dias for insightful discussions and suggestions. M.S. Ribeiro and M.S. Baptista thanks FAPESP (Grants 2010/13313-9; 2012/50680-5; 2013/07937-8), NAP-PhotoTec and CNPq for financial support.

Appendix A. Supplementary material

Supplementary data associated with this article can be found, in the online version, at http://dx.doi.org/10.1016/j.jphotobiol.2015.03.018.

References

[1] W.C. de Melo, P. Avci, M.N. de Oliveira, A. Gupta, D. Vecchio, M. Sadasivam, R. Chandran, Y.Y. Huang, R. Yin, L.R. Perussi, G.P. Tegos, J.R. Perussi, T. Dai, M.R. Hamblin, Photodynamic inactivation of biofilm: taking a lightly colored approach to stubborn infection, Expert Rev. Anti Infect Ther. 11 (2013) 669–693.
[2] F. Cieplik, L. Tabenski, W. Buchalla, T. Maisch, Antimicrobial photodynamic therapy for inactivation of biofilms formed by oral key pathogens, Front Microbiol. 5 (2014) 405.
[3] L. Huang, Y. Xuan, Y. Koide, T. Zhiyentayev, M. Tanaka, M.R. Hamblin, Type I and Type II mechanisms of antimicrobial photodynamic therapy: an in vitro study on gram-negative and gram-positive bacteria, Lasers Surg. Med. 44 (2012) 490–499.
[4] M. Wainwright, In defence of 'dye therapy', Int. J. Antimicrob. Agents 44 (1) (2014) 26–29.
[5] M. Wainwright, K.B. Crossley, Methylene blue–a therapeutic dye for all seasons?, J Chemother. 14 (2002) 431–443.
[6] J.P. Tardivo, A. Del Giglio, C.S. de, Oliveira, D.S. Gabrielli, H.C. Junqueira, D.B. Tada, D. Severino, R. de Fátima Turchiello, M.S. Baptista, Methylene blue in photodynamic therapy: from basic mechanisms to clinical applications, Photodiagnosis Photodyn. Ther. 2 (2005) 175–191.

[7] M.N. Usacheva, M.C. Teichert, M.A. Biel, The role of the methylene blue and toluidine blue monomers and dimers in the photoinactivation of bacteria, J. Photochem. Photobiol. B: Biol. 71 (2003) 87–98.
[8] H.C. Junqueira, D. Severino, L.G. Dias, M.S. Gugliotti, M.S. Baptista, Modulation of methylene blue photochemical properties based on adsorption at aqueous micelle interfaces, Phys. Chem. Chem. Phys. 4 (2002) 2320–2328.
[9] D. Severino, H.C. Junqueira, M. Gugliotti, M.S. Baptista, Influence of negatively charged interfaces on the ground and excited states properties of methylene blue, Photochem. Photobiol. 77 (2003) 459–468.
[10] S.C. Núñez, A.S. Garcez, I.T. Kato, T.M. Yoshimura, L. Gomes, M.S. Baptista, M.S. Ribeiro, Effects of ionic strength on the antimicrobial photodynamic efficiency of methylene blue, Photochem. Photobiol. Sci. 13 (2014) 595–602.
[11] B.J. Bennion, V. Daggett, The molecular basis for the chemical denaturation of proteins by urea, Proc. Natl. Acad. Sci. USA 100 (2003) 5142–5147.
[12] P. Mukerjee, A.K.J. Ghosh, The effect of urea on methylene blue, its self-association, and interaction with polyelectrolytes in aqueous solution, Phys. Chem. 67 (1963) 193–197.
[13] L.G. Dias, F.H. Florenzano, W.F. Reed, M.S. Baptista, S.M.B. Souza, E.B. Alvarez, H. Chaimovich, I.M. Cuccovia, C.L.C. Amaral, C.R. Brasil, L.S. Romsted, M.J. Politi, Effect of urea on biomimetic systems: neither water 3-d structure rupture nor direct mechanism, simply a more "polar water", Langmuir 18 (2002) 319–324.
[14] R. Itri, W. Caetano, L.R.S. Barbosa, M.S. Baptista, Effect of urea on bovine serum albumin in aqueous and reverse micelle environments investigated by small angle X-ray scattering, fluorescence and circular dichroism, Braz. J. Phys. 34 (2004) 58–63.
[15] B.D. Jett, K.L. Hatter, M.M. Huycke, et al., Simplified agar plate method for quantifying viable bacteria, Biotechniques 23 (1997) 648–650.
[16] M. Parrinello, A. Rahman, Polymorphic transitions in single crystals: a new molecular dynamics method, J. Appl. Phys. 52 (1981) 7182–7190.
[17] G. Bussi, D. Donadio, M. Parrinello, Canonical sampling through velocity rescaling, J. Chem. Phys. 126 (2007) 014101.
[18] H.J.C. Berendsen, J.P.M. Postma, W.F. van Gunsteren, J. Hermans, Interaction models for water in relation to protein hydration, in: B. Pullman (Ed.), In Intermolecular Forces, Reidel, Dordrecht, 1981, pp. 331–42.
[19] A.D. Becke, Density-functional exchange-energy approximation with correct asymptotic-behavior, Phys. Rev. A 38 (1988) 3098–3100.
[20] P.M.W. Gill, B.G. Johnson, J. Pople Michael, A. John, The performance of the Becke–Lee–Yang–Parr (B–LYP) density functional theory with various basis sets, Chem. Phys. Lett. 197 (1992) 499–505.
[21] I.C. Lin, M.D. Coutinho-Neto, C. Felsenheimer, O.A. von Lilienfeld, I. Tavernelli, U. Rothlisberger, Library of dispersion-corrected atom-centered potentials for generalized gradient approximation functionals: Elements H, C, N, O, He, Ne, Ar, and Kr, Phys. Rev. B 75 (2007) 205131.
[22] F. Bettanin, T.A.C. Fontinelles, L.G. Dias, M.D. Coutinho-Neto, P. Homem-de-Mello, Aggregation of photosensitisers: the role of dispersion and solvation on dimer formation energetics, 2014 (submitted for publication).
[23] C.M. Breneman, K.B. Wiberg, Determining atom-centered monopoles from molecular electrostatic potentials. The need for high sampling density in formamide conformational analysis, J. Comput. Chem. 11 (1990) 361–373.
[24] P. Stephens, F. Devlin, C. Chabalowski, M. Frisch, Ab initio calculation of vibrational absorption and circular dichroism spectra using density functional force fields, J. Phys. Chem. 98 (1994) 11623–11627.
[25] R. Krishnan, J.S. Binkley, R. Seeger, J.A. Pople, Self-consistent molecular orbital methods. XX. A basis set for correlated wave functions, J. Chem. Phys. 72 (1980) 650–654.
[26] B. Hess, H. Bekker, H.J.C. Berendsen, J.G.E.M. Fraaije, LINCS: a linear constraint solver for molecular simulations, J. Comput. Chem. 18 (1997) 1463–1472.
[27] T. Darden, D. York, L. Pedersen, Particle mesh Ewald: An N·log(N) method for Ewald sums in large systems, J. Chem. Phys. 98 (1993) 10089–10092.
[28] A. Leach, Molecular Modelling: Principles and Applications, Prentice Hall, New York, 2001.
[29] I.C. Lin, M.D. Coutinho-Neto, C. Felsenheimer, O.A. von Lilienfeld, I. Tavernelli, U. Rothlisberger, Library of dispersion-corrected atom-centered potentials for generalized gradient approximation functionals: elements H, C, N, O, He, Ne, Ar, and Kr, Phys. Rev. B 75 (2007) 205131.
[30] H.J.C. Berendsen, D. van der Spoel, R. van Drunen, GROMACS – a message-passing parallel molecular-dynamics implementation, Comput. Phys. Commun. 91 (1995) 43–56.
[31] E. Lindahl, B. Hess, D. van der Spoel, GROMACS 3.0: a package for molecular simulation and trajectory analysis, J. Mol. Model. 7 (2001) 306–317.
[32] M.J. Frisch, G.W. Trucks, H.B. Schlegel, G.E. Scuseria, M.A. Robb, J.R. Cheeseman, G. Scalmani, V. Barone, B. Mennucci, G.A. Petersson, et al., Gaussian 09, Gaussian Inc, Wallingford CT, 2009.
[33] S.C. Souza, J.C. Junqueira, I. Balducci, C.Y. Koga-Ito, E. Munin, A.O.C. Jorge, Photosensitization of different Candida species by low power laser light, J. Photochem. Photobiol. B: Biol. 83 (2006) 34–38.
[34] M. Wilson, N. Mia, Sensitization of *Candida albicans* to killing by low-power laser light, J. Oral. Pathol. Med. 22 (1993) 354–357.
[35] L.S. Peloi, R.R. Soares, C.E. Biondo, V.R. Souza, N. Hioka, E. Kimura, Photodynamic effect of light-emitting diode light on cell growth inhibition induced by methylene blue, J. Biosci. 33 (2008) 231–237.
[36] R.A. Prates, E.G. da Silva, A.M. Yamada Jr., L.C. Suzuki, C.P. Rodrigues, M.S. Ribeiro, Light parameters influence cell viability in antifungal photodynamic therapy in a fluence and rate fluence-dependent manner, Laser Phys. 19 (2009) 1038–1044.
[37] M.A. Castriciano, M. Samperi, S. Camiolo, A. Romeo, L.M. Scolaro, Unusual stepwise protonation and J-aggregation of meso-tetrakis(nmethylpyridinium-4-yl)porphine on binding poly(sodium vinylsulfonate), Chem. Eur. J. 19 (2013) 12161–12168.

Please cite this article in press as: S.C. Nuñez et al., Urea enhances the photodynamic efficiency of methylene blue, J. Photochem. Photobiol. B: Biol. (2015), http://dx.doi.org/10.1016/j.jphotobiol.2015.03.018